Contents list available at CBIORE journal website

International Journal of Renewable Energy Development

Journal homepage: https://ijred.cbiore.id

Research Article

Towards low-carbon and net-zero energy temperature control in winter cricket farming using a hybrid PV/T–heat pump system

Panuwit Puttaraksa, Thanyaluk Sundach, Sulaksana Mongkon, Chawaroj Jaisin, Sarawut Polvongsri*

Smart Energy and Environmental Research Unit (SEE-U), School of Renewable Energy, Maejo University, Chiang Mai, Thailand

Abstract. This study evaluated the integration of a photovoltaic–thermal (PV/T) system with a heat pump (HPs) to reduce energy consumption and carbon intensity in a community-scale cricket farming facility during the winter season. Two configurations were compared: a conventional HPs-only system and a hybrid HPs–PV/T system maintaining the rearing temperature at 28–30 °C. In the hybrid setup, a 10.8 kW_{th} heat pump served as the main heating unit, while eight 550 W_p PV/T panels supplied supplementary heat and electricity. The system performance was experimentally assessed, yielding an average heat-pump Coefficient of Performance (COP) of 3.13 and a PV/T performance ratio (PR) of 0.90 under winter conditions. The hybrid system reduced grid-electricity use to 1.58 kWh/day compared with 24.37 kWh/day in total consumption, achieving a 95.4% grid electricity displacement. Annually, the PV/T array generated 7,570.63 kWh of renewable energy—exceeding the total electricity demand of 7,369.07 kWh/yr. The organizational carbon-footprint analysis showed emissions declined from 5,025.98 kg CO_2e to 1,525.83 kg CO_2e, a 69 % reduction. Overall, the HPs–PV/T hybrid configuration proved to be an energy-efficient, low-carbon solution for temperature-controlled insect farming, particularly suitable for small- and community-scale applications.

Keywords: Heat pump; PV/T system; Cricket farming; Energy consumption; Carbon reduction

Received: 7th Nov 2025; Revised:20th Feb 2026; Accepted: 8th March 2026; Available online: 17th March 2026

1. Introduction

Northern Thailand is characterized by pronounced seasonal climatic variation, particularly during the winter months when ambient temperatures commonly decline to 12–20 °C (Thai Meteorological Department (TMD), 2023). Such suboptimal thermal conditions adversely affect agricultural production systems that are highly sensitive to environmental fluctuations. In particular, insect farming systems rely heavily on controlled microclimatic environments to maintain production efficiency and biological performance (FAO, 2021). Temperature is one of the most critical abiotic factors influencing insect physiology, as it directly affects metabolic activity, feed conversion efficiency, growth rate, and survival (Bawa *et al*, 2020; Booth & Kiddell, 2007). When insects are reared below their optimal thermal threshold, a decline in metabolic rates occurs, resulting in lower feed intake, prolonged development time, and reduced productivity (Lundy & Parrella, 2015). Consequently, these thermal constraints limit production cycles per year and increase the risk of yield instability, posing a major challenge to improving the productivity and economic competitiveness of insect farming in northern Thailand during the winter season (Halloran *et al*., 2017).

Temperature regulation is a critical factor directly influencing production efficiency in both livestock and insect farming systems, particularly those that rely on optimal feed-to-biomass conversion efficiency. In aquaculture, previous studies have demonstrated that maintaining species-specific thermal conditions significantly enhances biological performance. For example, Nile tilapia (Oreochromis niloticus) exhibited markedly improved growth rates and survival when reared at an optimal temperature of approximately 30 °C compared to sub-optimal thermal conditions (Mirea *et al*., 2013). Similarly, whiteleg shrimp (*Litopenaeus vannamei*) showed reduced survival at 30–32 °C, although growth performance peaked at around 28 °C (Wyban *et al*., 1995). In terrestrial livestock systems, temperature remains a dominant environmental variable affecting metabolic activity and feed utilization. Broiler chickens perform optimally within controlled thermal environments of 28–32 °C, minimizing cold-induced stress and supporting stable physiological function during winter conditions (Ajakaiye *et al*., 2011; Lin *et al*., 2006). Likewise, controlled-environment swine production recommends indoor temperatures ranging from 27–32 °C during the early finishing stage to sustain growth rates and improve feed conversion efficiency (National Research Council, 2012; Brown-Brandl *et al*., 2013). Studies in semi-confined beef cattle systems also reported that maintaining the rearing temperature above 28 °C reduces metabolic heat loss and improves growth performance (da Silva *et al*., 2017). Research in insect farming shows similar temperature sensitivity due to the ectothermic nature of insects. The survival rate of the lady beetle (*Harmonia axyridis*) declines significantly under low-temperature conditions around 22 °C

* Corresponding author
Email: sarawut_p@mju.ac.th (S. Polvongsri)

https://doi.org/10.61435/ijred.2026.61952
ISSN: 2252-4940/© 2026.The Author(s). Published by CBIORE

(Hiiesaar *et al*., 2001). Black soldier fly larvae (*Hermetia illucens*), widely used for organic waste bioconversion and alternative protein production, exhibit maximum biomass gain and shortest development time at 28–30 °C (Harnden & Tomberlin, 2016). The cowpea weevil (Callosobruchus maculatus) also shows delayed development at 20 °C compared to normal development at approximately 30 °C (Kutcherov, 2020). These findings are consistent with studies on the house cricket (*Acheta domesticus*), an economically important edible insect species, which thrives at 28–30 °C. This optimal temperature range enhances growth performance, reduces mortality, shortens rearing cycles, and achieves superior feed conversion ratios (FCR) (Halloran *et al*., 2017; Suckling *et al*., 2020). Overall, experimental evidence across multiple insect species confirms that the thermoneutral range of 27–32 °C supports maximum productivity, minimizes environmental stress, and reduces both feed and time inputs during rearing.

Previous studies have confirmed that temperature is a key environmental determinant of productivity in both livestock and insect farming, strongly affecting growth performance, survival, and feed-to-biomass conversion efficiency. In commercial rearing systems located in regions with low or fluctuating seasonal temperatures, artificial heating is essential to maintain optimal rearing conditions. However, conventional heating methods used in controlled-environment agriculture—such as electric heaters, hot-air blowers, and LPG systems—are highly energy-intensive. For example, space heating can account for up to 62% of total on-farm energy consumption (Zhang *et al*., 2021) and contributes significantly to greenhouse gas (GHG) emissions, reaching 4,300 $kgCO_2eq$ per greenhouse per year in fossil-fuel-based systems (Esen *et al*., 2013). Electric and LPG heating systems also emit 6,970 and 6,120 $kgCO_2eq$ annually, respectively, whereas applying thermal insulation or solar-assisted heating can reduce emissions by 18–35% (Decano-Valentin *et al*., 2021). More recently, hybrid renewable systems integrating photovoltaic/thermal (PV/T) collectors with heat pumps have been shown to reduce grid electricity consumption by up to 45% and lower GHG emissions by over 40% compared with conventional electric heating (Bae *et al*., 2022; Ntinas *et al*., 2014). In insect farming, thermal energy demand is also substantial. Cricket farms in the United Kingdom, for example, have reported annual emissions as high as 15,230 $kgCO_2eq$ per farm, with more than 60% originating from electricity use for heating and ventilation (Suckling *et al*., 2020). Although climate control improves productivity and reduces seasonal losses, it significantly increases energy consumption, highlighting the necessity of energy-efficient climate management strategies under the Organizational Carbon Footprint (CFO) framework.

Heat pumps, particularly air-source heat pumps (ASHPs), provide a high-efficiency alternative for agricultural heating applications due to their elevated coefficient of performance (COP = 3.0–4.5), which enables a 35–50% reduction in heating energy consumption compared with resistive electric or LPG-based heating systems (Ajakaiye *et al*., 2011). In this study, a heat pump was employed to generate hot water that was circulated through a heat exchanger integrated with the cricket rearing containers. When the ambient temperature dropped below the predefined threshold, the system activated an air circulation mechanism that directed air from the containers through the heat exchanger to maintain the optimal rearing temperature of 28–30 °C. However, despite its thermodynamic efficiency, the heat pump still requires electrical power input and therefore relies on grid electricity, resulting in indirect greenhouse gas (GHG) emissions. To address this limitation, renewable energy integration has been increasingly explored. In particular, hybrid photovoltaic–thermal (PV/T) systems coupled with heat pumps have emerged as a sustainable solution capable of simultaneously supplying thermal and electrical energy while reducing dependence on carbon-intensive grid power (Ajakaiye *et al*., 2011; Lin *et al*., 2006).

Consequently, this study aims to investigate the energy and environmental performance of a heat pump integrated with a solar photovoltaic–thermal (HPs-PV/T) system for controlled-environment cricket farming during winter in northern Thailand. The system simultaneously provides thermal energy to rearing containers and auxiliary electricity to reduce grid dependence, and its performance is evaluated under the Organizational Carbon Footprint (CFO) framework to quantify thermal and electrical performance, determine energy savings, and assess greenhouse gas emission reductions relative to a conventional heat-pump-only configuration.

2. Methods

2.1 Cricket rearing process

House crickets (*Acheta domesticus*) were used in the rearing system. The stocking density in each rearing container was maintained consistently throughout the experimental period to ensure stable biomass conditions. This control minimized the influence of variations in cricket biomass on the thermal load and energy consumption of the temperature control system.

The cricket rearing process can be divided into four main steps, as illustrated in Figure 1, with the details described as follows**:**

- Step 1: Procurement of eggs, feed, and egg trays through transportation. The eggs are then incubated for 7–10 days to allow hatching, producing coconut husk as waste.
- Step 2: Rearing crickets from the nymph stage to adulthood. Egg trays are placed in rearing ponds, and feed, water, and supplements are provided. Cricket excrement is generated as waste. During this process, air temperature is maintained at 28–30 °C using a combination of electricity-based heating, solar thermal energy, and a heat pump system, as illustrated in Figure 2(a) and Figure 2(b).
- Step 3: Harvesting crickets. The crickets are first stunned with cold water, followed by boiling using LPG gas. The harvested crickets are stored in refrigerated cabinets and

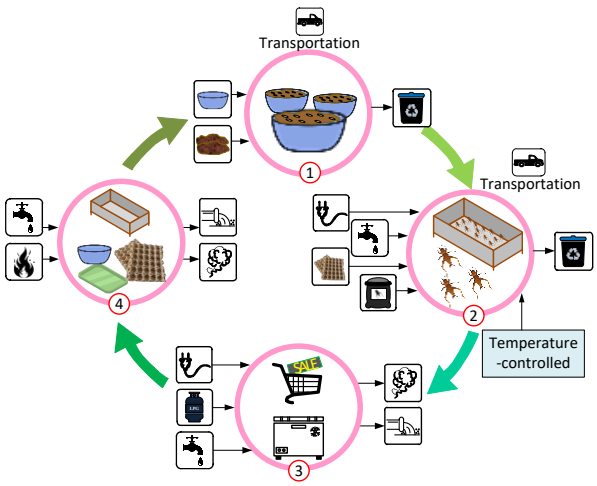

Fig 1. Cricket rearing process

then sold to enterprise groups. Waste generated includes wastewater and damaged egg trays after use.

- Step 4: Preparation of rearing ponds and equipment. The ponds are cleaned with water and detergent, containers for egg hatching are prepared, and reusable egg trays are baked at 60–70 °C for at least 30 minutes using charcoal as fuel.

2.2 System description

Temperature-controlled conditions in the cricket rearing containers were examined through two case studies, as illustrated in Figure 2(a). In the first configuration (Case HPs-only), a heat pump was employed as the sole thermal energy source for maintaining the desired temperature. In the second configuration (Case HPs–PV/T, shown in 2(b)), the heat pump was integrated with a solar photovoltaic–thermal system, which simultaneously supplied electrical and thermal energy to support the heating process. The detailed system configurations and operation principles of both cases are described in the following sections

Case HPs-only: Heat production and storage in hot water tank 1 are achieved using a heat pump. When electrical power from the grid is supplied, blower 1 draws ambient air through the evaporator coil. The refrigerant R410A inside the coil absorbs heat from the air and evaporates into a low-pressure vapor. This vapor is compressed, raising its pressure and temperature while maintaining its vapor phase. The high-temperature high-pressure vapor flows into the condenser while water pump 2 simultaneously circulates water from hot water tank 1 through the condenser. The water absorbs heat from the refrigerant, its temperature increases, and it is returned to the hot water tank for storage as usable hot water. After transferring heat to the water, the refrigerant condenses back into a high-pressure liquid. This liquid then passes through the expansion valve where its pressure and temperature decrease before returning to the evaporator to begin another cycle of heat absorption from the air. When the water temperature in hot water tank 1 reaches 55 °C the heat pump stops operating and when the water temperature drops below 32 °C the heat pump resumes operation. When the air temperature inside the cricket containers falls below 28 °C, hot water pump 2 delivers hot water to a heat exchanger integrated with the containers while blower 2 draws air across the exchanger until the air temperature rises above 30 °C at which point the system ceases operation.

In this study, a hierarchical temperature control strategy was implemented in which the heat pump operation is governed by the hot water tank temperature rather than the container air temperature. The hot water tank functions as a thermal buffer, decoupling heat production from heat demand within the cricket containers. The upper and lower temperature thresholds of 55 °C and 32 °C were selected to ensure sufficient thermal availability at the heat exchanger while minimizing excessive compressor cycling, particularly during periods of low ambient temperature. Although operating at higher storage temperatures may reduce instantaneous heat pump efficiency, this strategy improves operational stability and overall seasonal performance.

Case HPs-PV/T: The operating conditions of the heat pump and the air temperature control in the cricket containers were the same as in Case HPs-only. An additional system was introduced namely the use of a PV/T system as both a thermal energy source and an electricity generator to reduce the demand for grid electricity and to supplement the thermal energy provided in Case HPs-only. The PV/T system operates

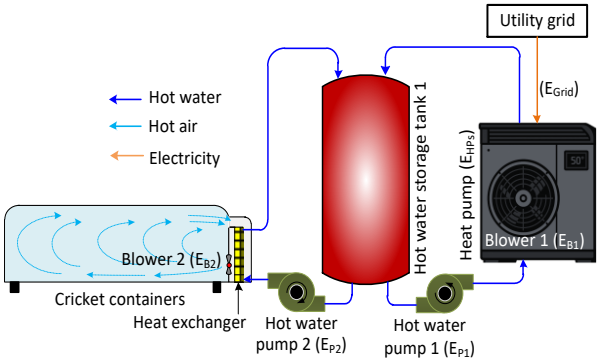

(a) Temperature control system from HPs-only

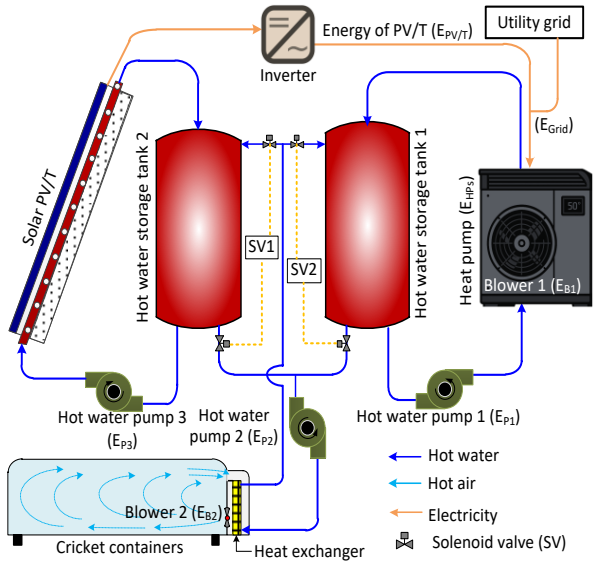

(b) Temperature controlled system from HPs-PV/T

Fig 2. Temperature control configurations for cricket rearing

by allowing the PV/T panels to absorb incoming solar radiation which increases the panel temperature. Water pump 3 circulates water to extract this heat raising the water temperature and storing it in hot water tank 2. At the same time part of the solar radiation is converted into electricity to supply the heat pump and the electrical loads within the farm. This combined approach effectively reduces the thermal load on the heat pump and lowers its electricity consumption.

It should be noted that the heat pump loop and the PV/T loop operate as independent hydraulic circuits with different mass flow rates. The heat pump loop circulates water through hot water tank 1 at a fixed mass flow rate optimized for stable compressor operation, while the PV/T loop circulates water through hot water tank 2 according to the collector design requirement expressed on an area basis (kg/s·m²). Thermal interaction between the two subsystems occurs through hot water storage and heat utilization at the container heat exchanger, rather than through direct hydraulic mixing. Therefore, the mass flow rates of the two loops are not required to be equal or synchronized.

As illustrated in Figure 2(a) and 2(b), the main components of the hybrid system for air temperature control in the cricket farming facility can be categorized into three subsystems: the heat pump system, the heat exchanger box and

Table 1
Technical specifications of the HPs–PV/T temperature control system

Subsystem	Component	Specification
Heat pump system	Refrigerant	R410A
	Heating capacity	10.8 kW
	Power consumption	2.8 kW
	Hot water storage tank-1	2,500 L
	Hot water pump 1	185 W
Heat exchanger & rearing unit	Heat exchanger box	0.8 m × 0.47 m
	Cricket containers	20 units (1.2 m × 2.4 m × 0.6 m each)
	Blower	3 units per container, 22 W each
	Hot water pump 2	374 W
PV/T system	PV/T module type	Monocrystalline half-cell
	Rated power	550 W per panel
	Collector area	2.57 m^2 per panel
	Number of panels	8 panels
	Inverter capacity	5.0 kW
	Hot water storage tank-2	1,000 L
	Hot water pump 3	374 W

cricket containers, and the PV/T system. The detailed specifications of each component are summarized in Table 1.

2.3 Energy demand estimation

2.3.1 Heat pump system performance

The performance of the heat pump system (HPs) was evaluated using experimentally measured data obtained from real-time monitoring during the winter rearing period. The analysis focused on the actual thermal energy output and corresponding electrical consumption. The instantaneous heating output of the HPs and the coefficient of performance (COP) were determined according to Equations (1)–(2). The daily and seasonal heating outputs were obtained by integrating the instantaneous heat production over the operating period, as expressed in Equation (3). The seasonal average COP represents the effective conversion efficiency of electricity into heat under local climatic conditions.

$$Q_{HPs}(t) = \dot{m}_{HPs} Cp_w \Delta T_{HPs}(t) \quad (1)$$

$$COP_{HPs}(t) = \frac{Q_{HPs}(t)}{P_{HPs}(t)} \quad (2)$$

$$Q_{HPs,daily} = \sum_{i=1}^{N} Q_{HPs}(t)\Delta t \quad (3)$$

Where: $\dot{m}_{HPs}$ is the mass flow rate of hot water circulated through the heat pump (0.28 kg/s), Cp_w is the specific heat capacity of water (4.187 kJ/kg·K), ΔT_{HPs} is the temperature rise of the water across the heat pump (K or °C), Q_{HPs} is the thermal output of the heat pump (kW_{th}), P_{HPs} is the total electrical input power of the heat pump system (kW_e), (including the compressor, blower 1 and hot water pump 2), COP_{HPs} is the coefficient of performance of the heat pump system, $Q_{HPs,daily}$ is the cumulative thermal output of the HP over the winter (MJ), N is the total number of measurement intervals, Δt is the measurement time step (s)

The total grid electricity consumption of the HPs-only system ($E_{grid,HPs\text{-}only}$) was determined by integrating the instantaneous power drawn by the heat pump from the grid throughout the operating period, as expressed in Equation (4).

$$E_{grid,HPs\text{-}only} = \sum (P_{HPs}(t)\Delta t) \quad (4)$$

2.3.2 Integration of HPs-PV/T

For the hybrid configuration, the PV/T module generates electricity to partially offset the grid electricity consumption of the HPs, while simultaneously providing hot water that supplements the thermal output of the HPs. This dual contribution reduces the net electricity demand and enhances the overall system efficiency.

The thermal output of the PV/T system was determined according to Equation (5).

$$\mathbf{Q_{PV/T}(t) = \dot{m}_{PV/T} Cp_w \Delta T_{PV/T}(t)} \quad (5)$$

The cumulative seasonal thermal contribution was obtained as:

$$\mathbf{Q_{PV/T,daily} = \sum_{i=1}^{N} Q_{PV/T}(t)\Delta t} \quad (6)$$

Where: $\dot{m}_{PV/T}$ is the mass flow rate of hot water circulated through the PV/T system (0.02 kg/s-m^2), $\Delta T_{PV/T}$ is the temperature rise of the water across the PV/T collector (K or °C), $Q_{PV/T}$ is the thermal output from the PV/T system (kW_{th})

The electrical energy produced by the PV/T module can be evaluated using Equation 7.

$$E_{PV/T} = \sum (P_{PV/T}(t_i)\Delta t) \quad (7)$$

Where: $E_{PV/T}$ is the electrical energy produced by PV/T during operation period (kWh), $P_{PV/T}$ is the electrical power output of PV/T (kW)

In addition to the thermal and electrical outputs, the electrical performance of the PV/T subsystem was evaluated using the performance ratio (PR), which represents the overall system efficiency under real operating conditions. The PR accounts for the effects of temperature, irradiance, and system losses, and was calculated according to the IEC 61724-1:2021 (International Electrotechnical Commission [IEC], 2021) standard, as expressed in Equation (8).

$$PR = \frac{Y_F}{Y_R} \quad (8)$$

where $Y_F = E_{PV/T}/P_{rated}$ is the final yield (kWh/kW_p) and $Y_R = H_t/G_{STC}$ is the reference yield (kWh/kW_p), with P_{rated} the

nominal installed PV capacity (4.4 kW_p), H_t the in-plane solar irradiation (kWh/m^2), and G_{STC} = 1 kW/m^2 the standard test irradiance. A higher PR value indicates better conversion performance and lower overall system losses, reflecting improved operational efficiency of the PV/T subsystem under actual climatic conditions.

The net grid electricity demand of the hybrid HPs–PV/T system ($E_{grid,HPs-PV/T}$) was determined by subtracting the electrical energy generated by the PV/T module from the total electricity consumed by the heat pump, as expressed in Equation (9). This represents the actual grid electricity required to operate the hybrid system.

$$E_{grid,HPs-PV/T} = \sum [P_{HPs}(t_i) - P_{PV/T}(t_i)]\Delta t \quad (9)$$

2.3.3 Energy saving potential and grid electricity reduction

The grid electricity reduction (GER) and energy saving potential (ESP) were introduced as key performance indicators to evaluate the effectiveness of PV/T integration in reducing grid electricity dependency. The GER quantifies the absolute reduction in grid-supplied electricity, while the ESP expresses this saving as a relative percentage compared with the HPs-only baseline. The grid electricity consumptions of both systems were obtained from Equations (4) and (9). The two indicators were then calculated using Equations (10) and (11).

$$GER = E_{grid,HPs-only} - E_{grid,HPs-PV/T} \quad (10)$$

$$ESP = \frac{E_{grid,HPs-only} - E_{grid,HPs-PV/T}}{E_{grid,HPs-only}} \times 100 \quad (11)$$

Although GER and ESP are derived from the same grid electricity consumption data, they represent different performance perspectives. GER indicates the absolute reduction in grid electricity consumption, whereas ESP expresses this reduction as a normalized indicator relative to the baseline system, allowing comparison across different operating conditions.

The renewable energy fraction (REF) was introduced to quantify the proportion of renewable energy supplied by the PV/T system relative to the total electricity consumption of the hybrid configuration. It represents the degree of self-sufficiency of the system and was determined according to Equation (12).

$$REF = \frac{E_{PV/T,annual}}{E_{HPs-PV/T,use}} \times 100 \quad (12)$$

Where $E_{PV/T,annual}$ is the total annual electricity generated by the PV/T array (kWh/yr), and $E_{HPs-PV/T,use}$ is the total annual electricity consumption of the heat pump system (kWh/yr).

It should be noted that the renewable energy fraction reflects the contribution of renewable electricity to the total system demand and does not represent the conversion efficiency of the system, which is evaluated separately using performance indicators such as COP.

2.4 Organizational carbon footprint assessment of a cricket farm

The Thailand Greenhouse Gas Management Organization (TGO) has established assessment guidelines in accordance with international standards, including ISO 14064-1 (International Organization for Standardization [ISO], 2018), the Greenhouse Gas Protocol (World Resources Institute [WRI] & World Business Council for Sustainable Development [WBCSD], 2001, 2004) (World Resources Institute (WRI) & World Business Council for Sustainable Development (WBCSD), 2001, 2004) and ISO/TR 14069 (International Organization for Standardization (ISO), 2013). These standards provide methodological guidance for quantifying, monitoring, and reporting organizational greenhouse gas emissions. The organizational carbon footprint assessment consists of three main steps as follows:

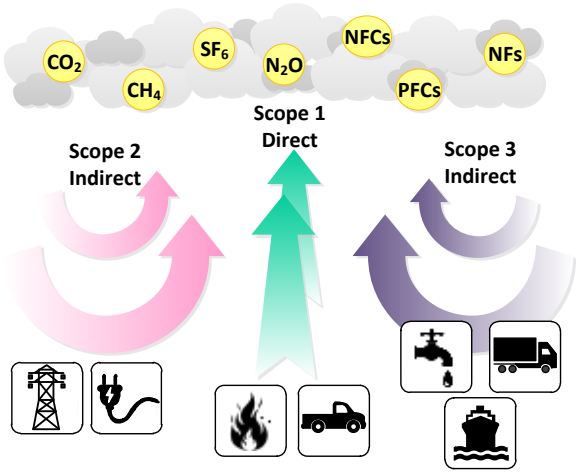

Fig. 4 Organizational carbon footprint boundary of the studied cricket farm

- Step 1: Defining the organizational boundary. The organizational boundary was determined using the control approach, and the assessment covered both greenhouse gas emissions and removals from the farm, with data collected between January and December 2024.
- Step 2: Defining the operational boundaries. The organizational carbon footprint assessment of the cricket farm was conducted at Kawinthida Farm, San Kamphaeng District, Chiang Mai Province. Activities contributing to greenhouse gas emissions were examined, and the emission sources were categorized into three types of scopes, as shown in Figure 4.
  - Scope 1: Direct emissions from sources owned or controlled by the cricket farm, including the on-site combustion of longan wood charcoal and liquefied petroleum gas (LPG) for boiling and processing crickets, as well as diesel fuel and Gasohol 91 used by farm-owned vehicles and equipment.
  - Scope 2: Indirect emissions from the consumption of electricity or thermal energy used in farm operations, such as ventilation fans, lighting, and other equipment, supplied either from purchased grid electricity or self-produced solar energy.
  - Scope 3: Other indirect emissions not included in Scope 1 and Scope 2, encompassing water consumption, landfilled waste, and transportation-related activities, including the outbound and return transportation of egg trays and cricket feed.
- Step 3: Calculation of greenhouse gas emissions and removals. The calculation of greenhouse gas (GHG) emissions and removals was performed using Activity Data (AD) and Emission Factors (EF). These factors are used to convert various farm activities into carbon dioxide equivalent (CO_2e) values. The assessment considered sources of GHG emissions and data collection, selecting appropriate GHG emission factors from the Thailand Greenhouse Gas Management Organization (TGO)

Table 2
The global warming potential (GWP)

Common name/ chemical formula	GWP100 values
Carbon dioxide (CO_2)	1
Methane (CH_4)	28
Fossil methane (CH_4)	30
Nitrous oxide (N_2O)	265
Hydrofluorocarbons (HFCs)	4-12,400
Perfluorocarbon (PFCs)	6,630-11,100
Sulfur hexafluoride (SF_6)	23,500
Nitrogen trifluoride (NF_3)	16,100

database. The calculation of greenhouse gas emissions was conducted as described in Equations 13 and 14.

$$GHG = \text{Emission data} \times GWP100 \quad (13)$$

$$GHG_{Emission} = AD \times EF \quad (14)$$

Where: GHG is the amount of greenhouse gas emissions, AD is activity data that generate greenhouse gas emissions, EF is emission factor for greenhouse gases

In this study, activity data for Scope 1 included the consumption of LPG, diesel fuel, Gasohol 91, and longan wood charcoal used in farm operations. Scope 2 emissions were calculated based on electricity consumption from farm equipment such as ventilation fans, lighting, and other electrical devices. Scope 3 emissions were estimated from indirect activities including water consumption, landfilled waste, and transportation of egg trays and cricket feed.

In the calculation, only greenhouse gases originating from anthropogenic (human) activities were considered. The global warming potential (GWP) over a 100-year time horizon (GWP_{100}) was applied to quantify the relative contribution of each greenhouse gas to climate change, following the methodological guidelines of the World Business Council for Sustainable Development (WBCSD) and the International Organization for Standardization (ISO) (World Resources Institute (WRI) & World Business Council for Sustainable Development (WBCSD), 2001), (International Organization for Standardization (ISO), 2013), as presented in Table 2.

CO_2 Emission reduction:

$$\Delta CO_2 = GER \times EF_{Grid} \quad (15)$$

where ΔCO_2 represents the reduction in CO_2 emissions, GER is the grid electricity reduction, and EF_{Grid} is the grid electricity emission factor obtained from the official Thailand grid emission factor published by the Thailand Greenhouse Gas Management Organization (Thailand Greenhouse Gas Management Organization (TGO), 2024).

2.5 Analysis of uncertainty and data quality

In preparing the data inventory for assessing the organizational carbon footprint of the cricket farm, the analysis of data uncertainty and quality is of critical importance, as it directly affects the reliability and accuracy of the overall assessment results. Scores can be assigned accordingly, and the scoring levels and criteria for evaluating uncertainty are presented in Table 3.

Table 3
Scoring criteria for emission factor (EF) data quality and associated uncertainty levels

Level	Score Range	Description
1	1-6	High uncertainty; poor data quality
2	7-12	Slight uncertainty; moderate data quality
3	13-18	Low uncertainty; good data quality
4	19-24	Low uncertainty; excellent data quality

- Characteristics of data collection

The quality of data can be divided into the following levels: X = 6 points, data collected continuously; Y = 3 points, data collected from meters and receipts; and Z = 1 point, data collected based on estimates (Intergovernmental Panel on Climate Change, 2006).

- Emission of greenhouse gases (EF)

The quality of emission factor (EF) data can be divided into the following levels: A = 4 points, EF obtained from high-quality measurements; B = 3 points, EF provided by manufacturers or national-level EF; C = 2 points, regional-level EF; and D = 1 point, global-level EF (Intergovernmental Panel on Climate Change, 2006).

3. Result and Discussion

3.1 System performance evaluation results

The daily test results show the relationship between solar radiation and ambient temperature during the period from 08:00 to 18:00 on 28 December 2024. The solar radiation started at about 156 W/m² at 08:00 and gradually increased to a maximum of 757 W/m² at noon before decreasing to nearly zero at 18:00. The average solar radiation throughout the day was about 477.54 W/m². The ambient temperature started at 20 °C and gradually increased following the change in solar radiation reaching a maximum of 30.70 °C at 13:00 before decreasing after 15:00. The average ambient temperature during the day was about 26.47 °C. These results indicate that the ambient temperature is directly related to the intensity of solar radiation due to the heat accumulation and release of the surrounding atmosphere and environment as shown in Figure 5

3.1.1 Experimental performance of the heat pump system

The performance characteristics of the heat pump system are illustrated in Figure 6. Figure 6 shows the operating performance of the heat pump system, including the variations of the coefficient of performance (COP_{HPs}), input power (P_{HPs}), and heat transfer rate at the condenser (Q_{HPs}) with respect to time. The heating capacity ranged between 9.96–10.44 kW_{th} throughout the operation period, indicating that the system maintained a stable heat transfer rate. The input power gradually increased from approximately 2.69 kW_e at the beginning to about 3.80 kW_e at the end of the test, reflecting the higher compressor demand as thermal energy accumulated in the system. As the hot water tank temperature increased, the electricity consumption of the heat pump also rose because the system was required to maintain heat transfer at the condenser against an increasing temperature difference. Consequently, the COP_{HPs} decreased from approximately 3.61 to about 2.67, with an average value of 3.13. These results demonstrate that the heat pump system was able to sustain stable heat transfer performance, while its energy efficiency gradually declined as

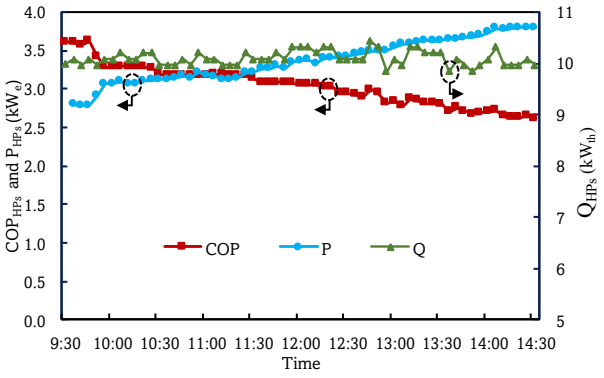

Fig 6. Performance of the heat pump system

the hot water tank temperature and cumulative operating time increased.

3.1.2 Experimental performance of the photovoltaic–thermal (PV/T) system

Figure 7 (a) illustrates the performance of the PV/T system in terms of electrical power, thermal output, and temperature difference across the PV/T panel. The electrical power output started at 0.5 kW_e at 08:00 and increased to a peak of 3.2 kW_e between 12:00 and 13:30 before gradually declining until 18:00, with a daily average of 2.1 kW_e. The thermal output began at 10:30 and varied with the temperature difference across the panel, reaching maximum values of 3.74 kW_{th} and 2.9 °C, respectively. The daily averages were 2.99 kW_{th} for thermal output and 2.32 °C for temperature difference, corresponding to a total daily thermal energy production ($Q_{PV/T\text{-}daily}$) of 51.21 MJ.

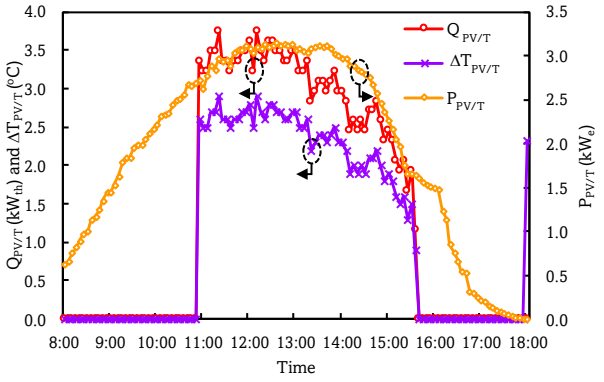

(a) Performance of the PV/T system

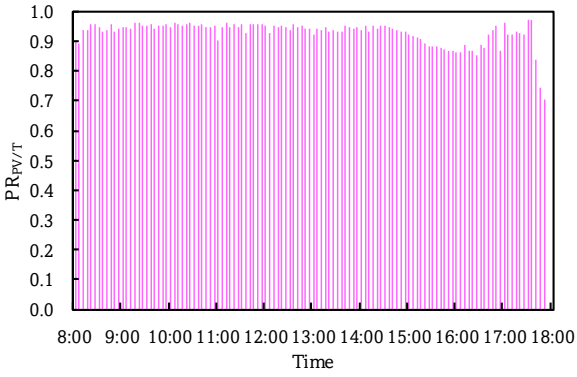

(b) Performance ratio

Fig 7. Experimental performance of the PV/T system

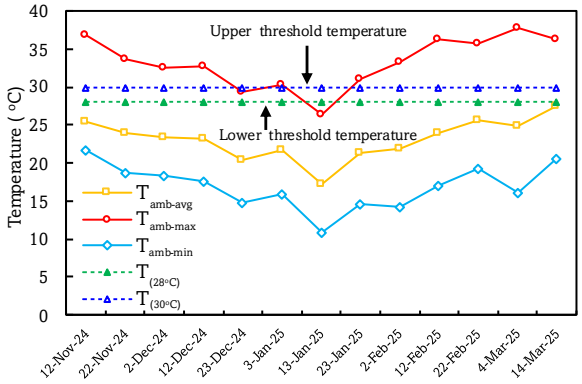

Fig 8. Daily variation of ambient air temperature from November 2024 to March 2025

The PR remained relatively stable throughout the operating period, with values close to unity, indicating efficient solar energy conversion. Both thermal output and temperature difference decreased over time as solar irradiance declined, consistent with the reduction in electrical power.

The performance ratio (PR) of the PV/T system, as shown in Figure 7 (b), remained at a high level from 08:00 to 15:00, ranging between 0.90 and 0.95. This period coincided with strong and stable solar irradiance, which enabled the photovoltaic cells to maintain efficient energy conversion. After 15:00, solar irradiance gradually declined due to changes in the angle of incidence and reduced radiation intensity. In addition, heat accumulation within the PV modules may have contributed to the decline in system performance. Consequently, the PR decreased to approximately 0.80–0.90 and eventually dropped to around 0.70. The average PR of the PV/T system was calculated as 0.90.

3.2 Experimental results during the winter season

3.2.1 Variation of air temperature in the winter period

Figure 8 shows the daily variation of ambient air temperature during the winter season from November 2024 to March 2025, comparing the maximum, average, and minimum values measured. The maximum temperature ranged from 26 to 38 °C, while the average and minimum values ranged from 18 to 27 °C and 11 to 22 °C, respectively. All values exhibited a decreasing trend from mid-November to mid-January before rising again during February and March 2025. Compared with the threshold range of 28–30 °C required to maintain suitable rearing conditions in 20 cricket containers, the minimum ambient temperature remained consistently below the lower limit, whereas the maximum temperature frequently exceeded the upper limit. This seasonal fluctuation directly affected the daily heating requirement of the temperature-controlled system ($Q_{HPs\text{-}only,daily}$) since lower ambient temperatures increased heat losses to the surroundings and required greater thermal energy input to sustain the target temperature inside the rearing containers.

3.2.2 Energy consumption for temperature-controlled during the winter season

Figure 9 (a) illustrates the variation of daily thermal output ($Q_{HPs\text{-}only,daily}$) and the corresponding grid electricity consumption ($E_{HPs\text{-}only,grid}$) for temperature control from November 2024 to March 2025. The results are consistent with

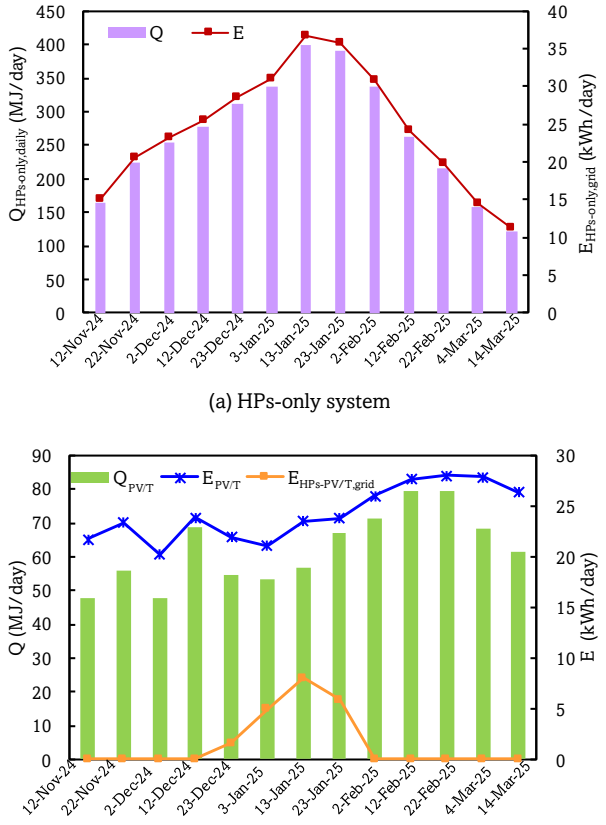

(a) HPs-only system

(b) Hybrid HPs–PV/T system

Fig 9. Daily thermal output and electrical energy consumption during the winter season for (a) the HPs-only system and (b) the hybrid HPs–PV/T system.

the ambient temperature profile shown in Figure 9. As the ambient temperature decreased during December and January, both the heating output and electrical consumption of the heat pump system increased significantly, reaching peak values of approximately 390.52 MJ/day and 35.80 kWh/day, respectively, in mid-January 2025. Conversely, during periods of higher ambient temperature from late February to March, both the required heating output and corresponding energy consumption gradually decreased. These results confirm that lower ambient temperatures lead to higher heating demand due to increased heat loss to the surroundings, whereas higher ambient temperatures reduce the heating load within the cricket rearing containers.

Figure 9 (b) shows the daily thermal output ($Q_{PV/T}$), electrical generation ($E_{PV/T}$), and net grid electricity consumption ($E_{HPs\text{-}PV/T,grid}$) of the hybrid PV/T system during the same period. Both thermal and electrical outputs of the PV/T subsystem gradually increased from December to February, reaching peak values of approximately 80 MJ/day for thermal energy and 28 kWh/day for electricity in late February 2025, corresponding to higher solar radiation levels during this period. In contrast, grid electricity consumption remained relatively low throughout most of the monitoring period and peaked only in mid-January 2025, when ambient temperatures were lowest and the heating load was highest. These results indicate that increased solar irradiance and ambient temperature enhanced the renewable energy contribution from the PV/T subsystem, thereby reducing both the heating requirement and the dependency on external grid electricity in the temperature-controlled cricket farming system.

Table 4
Average energy-saving performance of the hybrid system during the winter season

Variable	Value	unit
$E_{HPs\text{-}only,grid}$	24.37	[kWh/day]
$E_{HPs\text{-}PV/T,grid}$	1.58	[kWh/day]
GER	22.79	[kWh/day]
ESP	95.40	[%]

Table 4 summarizes the grid electricity displacement performance of the hybrid HPs–PV/T system during the winter season. The average daily electricity consumption of the heat pump with PV/T support ($E_{HPs–PV/T}$) was 24.37 kWh/day, while the electricity required from the grid ($E_{HPs–PV/T,grid}$) was only 1.58 kWh/day. Consequently, the displaced grid electricity reached 22.79 kWh/day, corresponding to a grid electricity displacement ratio of 95.4% compared with the HP-only configuration.

These results are consistent with the trends observed in Figure 11, where the combined thermal ($Q_{PV/T}$) and electrical ($E_{PV/T}$) outputs from the PV/T subsystem substantially reduced the reliance on grid electricity. The findings clearly demonstrate the effectiveness of the hybrid HPs–PV/T configuration in fulfilling the heating demand during the cold season while maintaining minimal grid dependency. This highlights the strong potential of the system to enhance energy efficiency and promote sustainable operation in temperature-controlled insect farming applications.

3.3 Annual energy production and consumption

The annual energy utilization of the HPs-only and HPs–PV/T systems is summarized in Table 5. Table 5 compares the annual energy performance of the HPs-only and HPs–PV/T systems. The hybrid configuration demonstrated complete independence from grid electricity. The total electricity consumption of the heat pump system was 7,001.75 kWh/yr, while the PV/T array generated 7,570.63 kWh/yr, as estimated using the RETScreen Expert software based on long-term, site-specific solar irradiation data (Natural Resources Canada, 2023). The lower annual electricity uses in the hybrid case compared with the HPs-only configuration, which consumed 7,369.07 kWh/yr, resulted from the additional thermal contribution

Table 5
Annual energy performance and grid-electricity saving of HPs-only and HPs–PV/T systems

Variable	HPs-only	HPs–PV/T	Unit
Q_{HPs}	44,599.42	37,127.01	[MJ/yr]
$Q_{PV/T}$	-	7,472.41	[MJ/yr]
$E_{HPs\text{-}only,annual}$	7,369.07	0	[kWh/yr]
$E_{HPs\text{-}PV/T,use}$	-	7,001.75	[kWh/yr]
$E_{PV/T,annual}$	-	7,570.63	[kWh/yr]
$E_{surplus}$	-	568.88	[kWh/yr]
GER_{annual}	-	7,369.07	[kWh/yr]
ESP_{annual}	-	100	[%]
REF	-	108.12	[%]

provided by the PV/T subsystem. The PV/T module delivered 7,472.41 MJ of useful heat annually, which reduced the thermal load on the heat pump and improved overall system efficiency. Moreover, the PV/T system produced a surplus of 568.88 kWh per year, indicating that it not only supplied all the required electricity for the heat pump but also generated excess renewable energy. Consequently, the hybrid system achieved an annual grid electricity reduction (GER_{annual}) of 7,369.07 kWh and an energy-saving potential (ESP_{annual}) of 100 %. In addition, the renewable energy fraction (REF) of the hybrid system was calculated as 108.12%, indicating that the annual renewable generation exceeded the total electricity consumption by approximately 8 %. This further confirms the system's full self-sufficiency and its capability to operate entirely on renewable energy without grid dependence. The combined thermal and electrical benefits of the hybrid system provide a strong foundation for assessing its CO_2 emission-reduction potential and highlight its environmental advantages for renewable-assisted temperature-controlled cricket farming.

3.4 Carbon footprint assessment

3.4.1 Input factors

Input factors related to energy and resource consumption were collected as activity data for the carbon footprint (CFO) assessment and categorized into Scope 1, Scope 2, and Scope 3 emission sources. The activity data collected for the greenhouse gas emission calculations are summarized in Table 6.

Based on Table 6, the assessment of input factors related to cricket rearing over a one-year period revealed the primary use of resources in energy, water, and transportation. For direct fuel consumption (Scope 1), the inputs included 20.10 kg of longan wood charcoal, 96.47 kg of liquefied petroleum gas (LPG), 10.78 L of diesel fuel, and 1.25 L of gasohol 91. These fuels are associated with direct production processes and internal transportation. For electricity consumption (Scope 2), two scenarios were examined. In the HPs-only system, all electricity was purchased from the grid, totaling 7,369.07 kWh per year, reflecting full dependence on external electricity supply. In the hybrid HPs-PV/T system, a total of 7,570.63 kWh per year was generated from solar energy, fully substituting the electricity that would otherwise be purchased from the grid (0 kWh). This demonstrates the potential of renewable energy use to completely reduce dependence on external electricity. For other indirect factors (Scope 3), water consumption totaled 80.39 m^3, waste for landfilling amounted to 436.35 kg, and transportation activities included the transport of cricket egg trays (88.56 tkm outbound, 12.65 tkm return) and cricket feed (78.24 tkm outbound, 11.18 tkm return). Overall, these data indicate that cricket rearing in the described system relies primarily on electricity, alongside the use of fuels, water, and transportation, all of which play a significant role in the overall production process.

3.4.2 Carbon footprint results

The greenhouse gas emissions assessment for cricket rearing in this study was divided into three scopes: Scope 1, direct fuel use; Scope 2, electricity consumption; and Scope 3, indirect activities such as water use, waste management, and transportation. Comparisons were made between the HPs-only system and the hybrid HPs-PV/T system. Detailed results are presented in Table 7.

Based on Table 7, it can be summarized that greenhouse gas emissions in the cricket rearing system originate from multiple factors. For Scope 1 (direct fuel use), the use of longan wood, liquefied petroleum gas (LPG), diesel fuel, and gasohol 91contributed a total of 336.69 $kgCO_2e$. Although this amount is not particularly high, it still highlights the need for more efficient fuel energy management, especially for LPG and diesel, which are fossil-based fuels.

For Scope 2 (electricity consumption), our system emitted 3,500.15 $kgCO_2e$, accounting for over 69% of total emissions in the HPs-only scenario. This underscores the significance of electricity management. Global analyses in agricultural systems highlight that Scope 2 emissions often dominate and that decarbonizing purchased energy is crucial in achieving net-zero pathways (Teske & Nagrath, 2022). In meat processing systems, Scope 2 constitutes a major share of carbon footprint and

Table 6
Input factors per year used for CFO calculation

Scope	Data list	Volume Sum	Source of evidence
Scope 1	Longan wood charcoal	20.10	Take notes
	LPG	96.47	Take notes
	Diesel fuel	10.78	Receipt
	Gasohol 91	1.25	Receipt
	The HPs-only system		
Scope 2	Electricity consumption – Purchased (Grid)	7,369.07	Monitoring system
	The hybrid HPs-PV/T system		
Scope 2	Electricity consumption – Self-produced (Solar)	7,001.75	Monitoring system
Scope 2	Electricity consumption – Purchased (Grid)	0	Monitoring system
Scope 3	Water consumption	80.39	Receipt
Scope 3	Landfilled waste	436.35	Take notes
Scope 3	Transportation of egg trays (Outbound)	88.56	Take notes
Scope 3	Transportation of egg trays (Return)	12.65	Take notes
Scope 3	Transportation of cricket feed (Outbound)	78.24	Take notes
Scope 3	Transportation of cricket feed (Return)	11.18	Take notes

Table 7
Greenhouse gas (GHG) emissions

Scope	Data list	Unit	Value	EF ($kgCO_2e$/Unit)	Total GHG ($kgCO_2e$)
Scope 1	Longan wood charcoal	kg	20.10	0.198	3.98
Scope 1	LPG	kg	96.47	3.113	300.31
Scope 1	Diesel fuel	L	10.78	2.74	29.55
Scope 1	Gasohol 91	L	1.25	2.2719	2.85
	Reduction of Greenhouse Gas Emissions in Scope 1 ($kgCO_2e$)				336.69
	The HPs-only system				
Scope 2	Electricity consumption – Purchased (Grid)	kWh	7,001.75	0.4999	3,500.15
	Reduction of Greenhouse Gas Emissions in Scope 2 ($kgCO_2e$)				3,500.15
	The hybrid HPs-PV/T system				
Scope 2	Electricity consumption – Self-produced (Solar)	kWh	8,258	0	-
Scope 2	Electricity consumption – Purchased (Grid)	kWh	-	0	-
	Reduction of Greenhouse Gas Emissions in Scope 2 ($kgCO_2e$)				-
Scope 3	Water consumption	m^3	80.39	0.541	43.49
Scope 3	Landfilled waste	kg	436.35	2.53	1,103.97
Scope 3	Transportation of egg trays (Outbound) 4-wheel pickup truck, 100% rugged performance, 100% Loading (maximum load weight 7 tons)	tkm	88.56	0.2154	19.08
Scope 3	Transportation of egg trays (Return) 4-wheel pickup truck, rugged driving, 0% Loading (maximum load weight 7 tons)	km	12.65	0.2415	3.06
Scope 3	Transportation of cricket feed (Outbound) 4-wheel pickup truck, 100% rugged performance, 100% Loading (maximum load weight 7 tons)	tkm	78.24	0.2154	16.85
Scope 3	Transportation of cricket feed (Return) 4-wheel pickup truck, rugged driving, 0% Loading (maximum load weight 7 tons)	km	11.18	0.2415	2.70
	Reduction of Greenhouse Gas Emissions in Scope 3 ($kgCO_2e$)				1,189.14
	Total Greenhouse Gas Emission Reduction in the HPs-only system ($kgCO_2e$)				5,025.98
	Total Greenhouse Gas Emission Reduction in the hybrid HPs-PV/T system ($kgCO_2e$)				1,525.83

strategies such as sourcing renewable electricity and adopting energy-efficient equipment have been shown to substantially lower emissions (Wróbel-Jędrzejewska, Włodarczyk, & Przybysz, 2025). For Scope 3 (indirect activities), water use, waste management, and transportation contributed a total of 1,189.14 $kgCO_2e$. The largest share originated from waste sent to landfill (1,103.97 $kgCO_2e$), indicating that waste from rearing is a key issue that should be managed to reduce environmental impacts. In contrast, emissions from transportation and water use were comparatively lower.

Considering the total emissions, the HPs-only system resulted in 5,025.98 $kgCO_2e$ (approximately 5.03 tCO_2e), whereas the combined use of the hybrid HPs-PV/T system reduced dependence on external electricity, lowering emissions to 1,525.83 $kgCO_2e$ (approximately 1.53 tCO_2e), representing a reduction of over 69% of total emissions. Similar reductions have been reported in agricultural and renewable-based systems (Huiran & Yiteng, 2025). Hybrid renewable systems designed for power generation also demonstrated significant CO_2 savings (Judijanto, 2025). Applications in greenhouse systems confirmed reduced grid dependence and associated emissions (Ates & Karaarslan, 2024).

These results indicate that integrating renewable energy systems, such as PV/T, with a heat pump not only reduces long-term energy costs but also significantly mitigates environmental impacts, particularly in production systems requiring continuous temperature control, such as closed-house cricket rearing. Furthermore, this approach aligns with the Sustainable Development Goals (SDGs), specifically climate action (SDG 13) and affordable and clean energy (SDG 7).

Based on proportional analysis, in the HPs-only system (as shown in Figure 10 (a)), the majority of greenhouse gas emissions originated from Scope 2 (electricity consumption), accounting for 69% of total emissions. This was followed by Scope 3 (24%), resulting from indirect activities such as transportation and waste management, while Scope 1 contributed only 7%. This highlights that reliance on electricity is the primary factor driving greenhouse gas emissions in this system. Conversely, when using the hybrid HPs-PV/T system (as shown in Figure 10 (b)), the proportion of Scope 2 dropped to 0%, indicating a complete elimination of dependence on external electricity. Consequently, emissions were limited to Scope 1 and Scope 3, with Scope 3 representing the largest share at 78% and Scope 1 at 22%, replacing the previously dominant role of electricity. This comparison demonstrates that integrating PV/T systems can significantly reduce grid electricity consumption and alter the structure of greenhouse gas emissions from electricity dependence to direct fuel use and

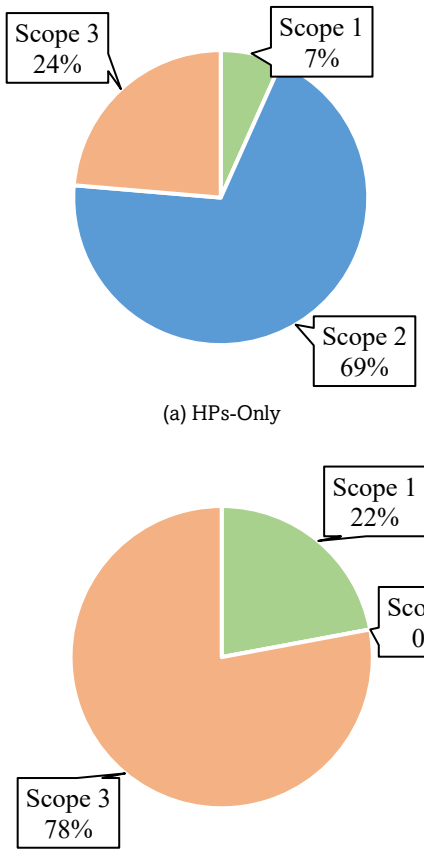

Fig 10. Proportion of total GHG emissions by scope (Scope 1, Scope 2, and Scope 3): (a) the HPs-only system, and (b) the hybrid HPs-PV/T system.

indirect activities. As a result, waste management and transportation become increasingly important considerations in renewable energy-based systems.

3.5 Data quality assessment by sources

The organizational carbon footprint assessment included verification and analysis of data quality according to established criteria, considering the sources of information, including handwritten notes, supporting documents such as receipts, and data from monitoring systems. These sources reflect varying levels of reliability and uncertainty. Table 8. presents the results of the data quality assessment for each activity according to the relevant Scope. The analysis of uncertainty and data quality in Section 2.5 indicates that each type of evidence corresponds to different levels of data quality, as follows:

- Monitoring system → High quality (X = 6 points) because the data are obtained directly from measurement instruments.
- Receipt → Medium quality (Y = 3 points) as the data are supported by purchase documents but not recorded in real time.
- Take notes → Lower quality (Z = 1 point) because the data are estimated or self-recorded and may contain uncertainties.

The results of the data quality assessment for each activity according to the relevant Scope are summarized in Table 8. Based on Table 8, the assessment results indicate that data obtained from the monitoring system was the highest quality, followed by receipts, while taking notes had the lowest quality. When the scores of all activities were combined, they fell within the range of 13–18 points, corresponding to Level 3, which means "low uncertainty and good data quality." This demonstrates that the data used for calculating the carbon footprint of the cricket farm is sufficiently reliable for analysis.

4. Conclusion

This study investigated the integration of a photovoltaic–thermal (PV/T) system with a heat pump (HPs) to reduce energy consumption and carbon intensity in a community-scale cricket farming facility during the winter season, where the air temperature of 20 cricket containers was maintained at 28–30 °C. The PV/T system demonstrated stable and efficient

Table 8
Assessment of data quality based on source

Scope	Data list	Volume	Source of evidence	Quality Level	Score
Scope 1	Longan wood charcoal	20.10	Receipt	Y	3
Scope 1	LPG	96.47	Receipt	Z	3
Scope 1	Diesel fuel	10.78	Receipt	Y	3
Scope 1	Gasohol 91	1.25	Receipt	Y	3
Scope 2 (Heat pump only)	Electricity consumption – Purchased (Grid)	7,002	Monitoring system	X	6
Scope 2 (Heat pump with PVT)	Electricity consumption – Self-produced (Solar)	8,258	Monitoring system	X	6
Scope 2 (Heat pump with PVT)	Electricity consumption – Purchased (Grid)	0	Monitoring system	X	6
Scope 3	Water consumption	80.39	Monitoring system	Y	6
Scope 3	Landfilled waste	436.35	Receipt	Y	3
Scope 3	Transportation of egg trays (Outbound)	88.56	Receipt	Y	3
Scope 3	Transportation of egg trays (Return)	12.65	Receipt	Y	3
Scope 3	Transportation of cricket feed (Outbound)	78.24	Receipt	Y	3
Scope 3	Transportation of cricket feed (Return)	11.18	Receipt	Y	3

performance, producing peak outputs of 3.20 kW_e and 3.74 kW_{th} with a daily thermal energy production of 51.21 MJ, while maintaining an average performance ratio (PR) of 0.90, which was used for annual energy yield estimation. The heat pump also showed stable operation, maintaining a heat transfer rate of 9.96–10.44 kW_{th} with an average coefficient of performance (COP) of 3.13.

The hybrid HPs–PV/T configuration significantly reduced grid electricity consumption during the winter period. The average electricity consumption of the heat pump was 24.37 kWh/day, while grid electricity demand was reduced to only 1.58 kWh/day, corresponding to a displaced grid electricity of 22.79 kWh/day or a grid electricity displacement ratio of 95.40% compared with the HPs-only system. In addition, the hybrid system achieved full energy self-sufficiency, generating 7,570.63 kWh per year, which exceeded the annual electricity demand of 7,369.07 kWh. This resulted in a renewable energy fraction of 108.12% and enabled zero grid-electricity consumption throughout the year. Furthermore, the carbon footprint assessment revealed that greenhouse gas emissions decreased from 5,025.98 $kgCO_2e$ in the HPs-only system to 1,525.83 $kgCO_2e$ in the hybrid HPs–PV/T system, representing a reduction of approximately 69%. The monitoring system also demonstrated high data quality, with overall scores of 13–18 points (Level 3), indicating low uncertainty and reliable results for the carbon footprint assessment.

Acknowledgments

This study was funded by School of Renewable Energy and Maejo University for the project to produce and develop graduates in renewable energy for ASEAN countries for graduate students (2023) and The authors would like to express a deep gratitude to The Agricultural Research Development Agency (Public Organization) provided funding for the project Temperature and weather control system for increasing productivity in Cricket farming using Solar Photovoltaic/Thermal (Solar-PVT) heat pump technology. The authors would also like to express an appreciation to School of Renewable Energy, Maejo University for the assistance and support.

Author Contributions: P.P.: Conceptualization, Data curation, Formal analysis, Methodology and Writing – review & editing. T.S.; Data curation and Methodology. C.J.; Data curation and Methodology. S.M.; Data curation and Methodology. S.P.; Data curation, Methodology Supervision, Validation and Writing – review & editing. All authors have read and agreed to the published version of the manuscript.

Funding: This research was financially supported by the Agricultural Research Development Agency (Public Organization), Thailand, under project number PRP6705030680, awarded to Sarawut Polvongsri (corresponding author). The first author, Panuwit Puttaraksa, gratefully acknowledges the scholarship support for tuition fees from the School of Renewable Energy, Maejo University, Chiang Mai, Thailand.

Conflicts of Interest: The authors declare that they have no known competing financial interests or personal relationships that could have appeared to influence the work reported in this paper.

References

Ajakaiye, J. J., Ayo, J. O., & Ojo, S. A. (2011). Effects of heat stress on some blood parameters and egg production of Shika Brown layer hens transported by road. *Biological Research*, 44(2), 163–167. https://doi.org/10.4067/s0716-97602010000200006.

Ates, E., & Karaarslan, N. (2024). Investigation of hybrid renewable energy green house for reducing residential carbon emissions. *International Journal of Thermofluids*, 21, 100558. https://doi.org/10.1016/j.ijft.2023.100558.

Bae, S., Chae, S., & Nam, Y. (2022). Performance analysis of integrated photovoltaic-thermal and air source heat pump system through energy simulation. *Energies,* 15(2), 528. https://doi.org/10.3390/en15020528.

Bawa, M., Songsermpong, S., Kaewtapee, C., & Chanput, W. (2020). Effect of diet on the growth performance, feed conversion, and nutrient content of the house cricket. *Journal of Insect Science,* 20(2), 10. https://doi.org/10.1093/jisesa/ieaa014.

Booth, D. T., & Kiddell, K. (2007). Temperature and the energetics of development in the house cricket (Acheta domesticus). *Journal of insect physiology*, 53(9), 950-953. https://doi.org/10.1016/j.jinsphys.2007.03.009.

Brown-Brandl, T. M., Eigenberg, R. A., & Nienaber, J. A. (2013). Heat stress risk factors of feedlot heifers. *Livestock Science*, 152(2–3), 190–198. https://doi.org/10.1016/j.livsci.2006.04.025.

da Silva, R. G., Maia, A. S. C., & de Macedo Costa, L. L. (2017). Index of thermal stress for dairy cows (ITSC) under high solar radiation in the northeast region of Brazil. *Journal of Thermal Biology*, 66, 20–28. https://doi.org/10.1007/s00484-014-0868-7.

Decano-Valentin, C., Lee, I. B., Yeo, U. H., Lee, S. Y., Kim, J. G., Park, S. J., ... & Jeong, H. H. (2021). Integrated building energy simulation–life cycle assessment (Bes–lca) approach for environmental assessment of agricultural building: A review and application to greenhouse heating systems. *Agronomy,* 11(6), 1230. https://doi.org/10.3390/agronomy11061230.

Esen, M., & Yuksel, T. (2013). Experimental evaluation of using various renewable energy sources for heating a greenhouse. *Energy and Buildings,* 65, 340-351. https://doi.org/10.1016/j.enbuild.2013.06.018.

FAO. (2021). Edible insects: Future prospects for food and feed security. Food and Agriculture Organization. https://www.fao.org/4/i3253e/i3253e.pdf.

Halloran, A., Roos, N., Eilenberg, J., Cerutti, A., & Bruun, S. (2016). Life cycle assessment of edible insects for food protein: a review. *Agronomy for Sustainable Development*, 36(4), 57. https://doi.org/10.1007/s13593-016-0392-8.

Harnden, L. M., & Tomberlin, J. K. (2016). Effects of temperature and diet on black soldier fly, Hermetia illucens (L.) (Diptera: Stratiomyidae), development. *Forensic Science International,* 266, 109-116. https://doi.org/10.1016/j.forsciint.2016.05.007.

Hiiesaar, K., Metspalu, L., Jõgar, K., & Kuusik, A. (2001). Influence of low temperature on survival of ladybird beetle (Harmonia axyridis). *Agronomy Research,* 2(1), 41–52. https://www.agronomy.emu.ee/vol02Spec/p02s05.pdf.

Huiran, L. & Yiteng, L. (2025). Agricultural carbon footprints, renewable energy and ecological footprint in agriculture. *Scientific Reports*, 15, 34429. https://doi.org/10.1038/s41598-025-18634-0.

Intergovernmental Panel on Climate Change. (2006). 2006 IPCC guidelines for national greenhouse gas inventories: Volume 1, general guidance and reporting. *Institute for Global Environmental Strategies (IGES).* https://www.ipcc-nggip.iges.or.jp/public/2006gl/vol1.html.

International Electrotechnical Commission (IEC). (2021). IEC 61724-1:2021 — Photovoltaic system performance – Part 1: Monitoring (2nd ed.). Geneva, Switzerland: IEC. https://www.iec.ch/homepage.

International Organization for Standardization (ISO). (2013). ISO/TR 14069:2013 — Greenhouse gases — Quantification and reporting of greenhouse gas emissions for organizations — Guidance for the application of ISO 14064-1. Geneva: ISO. https://www.iso.org/standard/43263.html.

International Organization for Standardization (ISO). (2018). ISO 14064-1:2018 — Greenhouse gases — Part 1: Specification with guidance at the organization level for quantification and reporting of greenhouse gas emissions and removals. Geneva: ISO. https://www.iso.org/standard/66453.html.

Judijanto L. (2025). Hybrid renewable energy system: Sustainable energy engineering solutions for the future. *Journal of Renewable Engineering*. 2(2). https://doi.org/10.62872/h7jjzb68.

Kutcherov, D. (2020). Stagewise resolution of temperature-dependent embryonic and postembryonic development in the cowpea seed beetle Callosobruchus maculatus (F.). *BMC ecology,* 20(1), 50. https://doi.org/10.1186/s12898-020-00318-2.

Lin, H., Jiao, H. C., Buyse, J., & Decuypere, E. (2006). Strategies for preventing heat stress in poultry. *World's Poultry Science Journal,* 62(1), 71–86. https://doi.org/10.1079/wps200585.

Lundy, M. E., & Parrella, M. P. (2015). Crickets are not a free lunch: protein capture from scalable organic side-streams via high-density populations of Acheta domesticus. *Journal of Cleaner Production.* https://doi.org/10.1371/journal.pone.0118785.

Mirea, C., Cristea, V., Grecu, I. R., & Dediu, L. (2013). Influence of different water temperature on intensive growth performance of Nile tilapia (Oreochromis niloticus, Linnaeus, 1758) in a recirculating aquaculture system. *Lucrări Ştiinţifice – Seria Zootehnie,* 60, 218–221. https://www.cabidigitallibrary.org/doi/full/10.5555/20143207790.

National Research Council, Division on Earth, Life Studies, & Committee on Nutrient Requirements of Swine. (2012). Nutrient requirements of swine. Washington, DC: National Academies Press. https://doi.org/10.17226/13298.

Natural Resources Canada. (2018). RETScreen Expert software, version 8. Minister of Natural Resources Canada, Ottawa, Canada. https://www.nrcan.gc.ca/maps-tools-and-publications/tools/modelling-tools/retscreen/7465.

Ntinas, G. K., Fragos, V. P., & Nikita-Martzopoulou, C. (2014). Thermal analysis of a hybrid solar energy saving system inside a greenhouse. *Energy Conversion and Management*, 81, 428-439. https://doi.org/10.1016/j.enconman.2014.02.058.

Suckling, J., Druckman, A., Moore, C. D., & Driscoll, D. (2020). The environmental impact of rearing crickets for live pet food in the UK, and implications of a transition to a hybrid business model combining production for live pet food with production for human consumption. *The International Journal of Life Cycle Assessment*, 25(9), 1693-1709. https://doi.org/10.1007/s11367-020-01778-w.

Thai Meteorological Department (TMD). (2023). Climate of Northern Thailand. Bangkok, Thailand. https://www.tmd.go.th.

Thailand Greenhouse Gas Management Organization (TGO). (2024). Thailand grid electricity emission factor. Bangkok, Thailand. https://www.tgo.or.th.

World Resources Institute (WRI) & World Business Council for Sustainable Development (WBCSD). (2001). The Greenhouse Gas Protocol: A corporate accounting and reporting standard. Washington, DC: WRI/WBCSD. https://ghgprotocol.org/sites/default/files/standards/ghg-protocol-revised.pdf.

World Resources Institute (WRI) & World Business Council for Sustainable Development (WBCSD). (2004). The Greenhouse Gas Protocol: A corporate accounting and reporting standard (revised edition). Washington, DC: WRI/WBCSD. https://ghgprotocol.org/sites/default/files/standards/ghg-protocol-revised.pdf.

Wróbel-Jędrzejewska, M., Włodarczyk, E., & Przybysz, Ł. (2025). Carbon footprint analysis for Scope 1 and 2 in meat production–Case study of polish plants. *Food and Bioproducts Processing*, 151, 327-336. https://doi.org/10.1016/j.fbp.2025.04.003.

Wyban, J., Walsh, W. A., & Godin, D. M. (1995). Temperature effects on growth, feeding rate and feed conversion of the Pacific white shrimp (Penaeus vannamei). *Aquaculture,* 138(1-4), 267-279. https://doi.org/10.1016/0044-8486(95)00032-1.

Zhang, F., Liu, F., Ma, X., Guo, G., Liu, B., Cheng, T., ... & Wang, X. (2021). Greenhouse gas emissions from vegetables production in China. *Journal of Cleaner Production*, 317, 128449. https://doi.org/10.1016/j.jclepro.2021.128449.